CrossMark

REVIEW

On sorption and swelling of CO_2 in clays

**A. Busch · P. Bertier · Y. Gensterblum · G. Rother ·
C. J. Spiers · M. Zhang · H. M. Wentinck**

Abstract The geological storage of carbon dioxide
(CO_2) is a well-studied technology, and a number of
demonstration projects around the world have proven
its feasibility and challenges. Storage conformance
and seal integrity are among the most important
aspects, as they determine risk of leakage as well as
limits for storage capacity and injectivity. Further-
more, providing evidence for safe storage is critical
for improving public acceptance. Most caprocks are
composed of clays as dominant mineral type which
can typically be illite, kaolinite, chlorite or smectite.
A number of recent studies addressed the interaction
between CO_2 and these different clays and it was
shown that clay minerals adsorb considerable quan-
tities of CO_2. For smectite this uptake can lead to
volumetric expansion followed by the generation of
swelling pressures. On the one hand CO_2 adsorption
traps CO_2, on the other hand swelling pressures can
potentially change local stress regimes and in
unfavourable situations shear-type failure is assumed
to occur. For storage in a reservoir having high clay
contents the CO_2 uptake can add to storage capacity
which is widely underestimated so far. Smectite-rich
seals in direct contact with a dry CO_2 plume at the
interface to the reservoir might dehydrate leading to
dehydration cracks. Such dehydration cracks can
provide pathways for CO_2 ingress and further accel-
erate dewatering and penetration of the seal by
supercritical CO_2. At the same time, swelling may
also lead to the closure of fractures or the reduction
of fracture apertures, thereby improving seal integ-
rity. The goal of this communication is to theoreti-
cally evaluate and discuss these scenarios in greater
detail in terms of phenomenological mechanisms, but
also in terms of potential risks or benefits for carbon
storage.

Keywords CCS · CO_2 storage · Clay swelling ·
Carbon dioxide · Leakage · Containment · Smectite

A. Busch (✉) · H. M. Wentinck
Shell Global Solutions International B.V., Kessler Park 1,
2288 GS Rijswijk, The Netherlands
e-mail: andreas.busch@shell.com

P. Bertier
Energy and Mineral Resources Group, Clay and Interface
Mineralogy, RWTH Aachen University, Bunsenstr. 8,
52072 Aachen, Germany

Y. Gensterblum
School of Earth, Energy and Environmenal Sciences,
Stanford University, Stanford, CA, USA

G. Rother
Chemical Sciences Division, Oak Ridge National
Laboratory, Oak Ridge, TN 37830-6110, USA

C. J. Spiers · M. Zhang
Department of Earth Sciences (HPT Lab), Utrecht
University, Budapestlaan 4, 3584 CD Utrecht,
The Netherlands

1 Introduction

For the characterization of geological CO_2 storage reservoirs, a number of critical parameters need to be assessed. From existing knowledge and experience, especially collected in the oil and gas industry, the storage capacity and injection rate are generally well understood for specific reservoirs. Critical parameters are reservoir size and reservoir heterogeneity, i.e. porosity and (relative) permeability, fluid saturation, the reservoir stress field, in particular the minimum horizontal stress, as well as pressure and temperature conditions.

In addition, the identification and risk assessment of potential leakage pathways, reservoir depletion rate in case of leakage and reservoir pressure at which leakage is initiated or inhibited, are unique to a CCS project and thus need to be considered. Pressure is a key parameter in any leakage scenario, and will decrease in typical fluid extraction processes but increase in storage applications. The CO_2 injected into a reservoir may, sometimes significantly, increase the average reservoir pressure. Initially, pressure builds up only locally, i.e. in the vicinity of the injection well. Imperfections in cementation of injection, monitoring or abandoned wells, can result in the formation of micro-annuli between cement and caprock or cement and casing, potentially acting as pathways for gas leakage. With continuing injection, the pressure pulse will eventually be transmitted to the far field. The resulting rise of the reservoir pore pressure reduces the effective stress on existing fractures and faults, potentially causing their (re)activation.

The main trapping mechanisms in CO_2 storage are structural and residual trapping. In structural trapping, a continuous, connected gas column will form underneath a sealing formation. Buoyancy results in fluid pressure acting on the reservoir-caprock interface, which must be lower than the capillary entry pressure of the seal to prevent capillary leakage. Hence, this maximum pressure or gas column height is a key parameter in the assessment of a storage scenario. In residual trapping, gas resides in disconnected bubbles in pores and is therefore not contributing to a buoyancy pressure.

The factors controlling leakage from a gas storage reservoir have been addressed earlier for a range of applications. Yet, the specific properties of CO_2 add to the complexity of the assessment of leakage scenarios. For instance, CO_2 dissolves in brine or water, forms a weak acid and possibly reacts with surrounding rock surfaces. While many of these reactions are probably rather insignificant within the time scales of interest (<10,000 years), the dissolution or precipitation of carbonates and sulfates might occur within relevant time scales. In addition, CO_2 exhibits specific wetting behaviour, and incomplete water-wetting conditions have been reported. Moreover, wetting properties may be altered by water–rock-interactions (Iglauer et al. 2015), potentially affecting two-phase flow in the reservoir and capillary sealing of barriers.

CO_2 also interacts with the nanopores of shales, which largely consist of clay minerals, by diffusion through the aqueous phase or drainage of water from the pore space and subsequent adsorption on the high surface area clays. In the last 5–10 years, a series of studies (Busch et al. 2008; Loring et al. 2011; Rother et al. 2013a; Schaef et al. 2012; Weniger et al. 2010, amongst others) reported on this interaction, with a major focus on swelling clays, such as montmorillonite (MMT). It was found that for CO_2 storage containment, non-negligible physical effects result from reacting clays with CO_2 at hydrostatic pressure, temperature, and stress conditions representative of geological reservoirs.

The aim of this contribution is to provide a summary of these studies, and to put them into perspective with regards to the geological storage of CO_2. We present a brief literature review, followed by detailed discussions of several storage scenarios in which CO_2-clay interactions may play a role and affect sealing efficiency of caprocks and wells. The potential of CO_2-clay interactions for CO_2 trapping is discussed. Temperature and pressure changes in the reservoir affect local and reservoir stresses. These are standard reservoir management issues relevant in many different improved or enhanced production operations and need to be addressed in the geomechanical evaluation of any Carbon Capture and Storage (CCS) project.

1.1 Clay minerals in geological reservoirs

Before addressing the interactions between CO_2, water, and clay minerals, with a specific focus on smectite, it is helpful to review the stability of clays in the sub-surface at the specific pressures, temperature and chemical conditions relevant for geological reservoirs. A general overview on clay classification and physico-chemical properties is provided in Bergaya et al. (2006), amongst others. Smectite is a low-charge, expandable clay. Its

basic structure consists of a 10 Å layer composed of an octahedral sheet sandwiched between 2 tetrahedral sheets (TOT structure), plus the pore space (interlayer space) between such TOT structures. This interlayer space is expandable, depending on hydration state, i.e. the amount of water layers confined in this space. During sediment burial, smectite commonly convert into illite by passing through a transition phase characterized by smectite-illite mixed layers. Different models have been discussed for this reaction, and an overview of this work is provided in e.g. Altaner and Ylagan ([1997]). The smectite-to-illite transition depends on a range of factors like temperature, geologic time, porosity and permeability, connectivity between formations, formation water chemistry, and water/rock ratio. All these factors are oftentimes constantly changing with basin history. The entire process is complex but has important implications for many aspects like geo-pressurization, the growth of fault and fracture zones, or hydrocarbon migration. More details are given in Altaner and Ylagan ([1997]), Brigatti et al. ([2013]), Ferrage et al. ([2011]) and Lanson et al. ([2009]). Clay minerals (e.g. illite, smectite, kaolinite, chlorite) typically occur in every sedimentary basin, no matter what the reservoir conditions are. Expansion of clays was, however, mainly observed for smectite (exceptions apply), and we therefore briefly discuss the stability of smectite in relation to the above mentioned smectite-to illite-transformation. In geological reservoirs the controlling factor for the transition from pure smectite to illite, through an illite/smectite (I/S) mixed-layer transition stage, can be temperature. Several studies investigated the relative smectite content in I/S mixed-layers, and found that for a sedimentary basin with a geothermal gradient of 25–35 °C/km, smectite content decreases to 20 % or even less, assuming that at temperatures of ∼120–175 °C the transformation is complete. This corresponds to a burial depth of at least 4–6 km (e.g. Hower et al. [1976]; Lanson et al. [2009]; Velde and Vasseur [1992]) and gives constraints on the occurrence of swelling clays in sedimentary basins, and hence within tight argillaceous rocks overlying CO_2 storage reservoirs. Especially deeply buried reservoirs, that underwent inversion resulting in present day depths of 1–3 km, will have had most or even all of their initial smectite content transformed to illite. Such depths are considered to be good candidates for CO_2 storage due to high CO_2 densities at moderate depths, keeping drilling costs low. A summary of clay mineralogy and smectite

contents of the different CO_2 storage operations around the world is given by Espinoza and Santamarina ([2012]). Clay contents, when mudrocks represent the primary caprock, are usually 50 % and higher. Smectite contents however are usually small with values of up to 9 % (Sleipner, Norway), or 1–3 % (Otway, Australia). High I/S mixed layers contents have been reported for the SACROC (up to 62 %) and Frio (45 %) projects, both in the USA (Espinoza and Santamarina [2012]). Smectite contents within the mixed-layers were not determined. Irrespective of these observations, young subsiding basins, like many reservoirs in the North Sea or the Gulf of Mexico, can show significant amounts of smectite or I/S mixed layers, and are hence subject to interactions with CO_2 as will be discussed in the following.

1.2 CO_2 sorption on clay minerals

Many studies published recently focus on the physical interactions between CO_2 and clay minerals. The goal of these papers was to better understand the response of clays in contact with CO_2, and to relate this information to subsurface conditions for the geological storage of CO_2. Earlier work on CO_2 sorption on clays (e.g., Fripiat et al. [1974]) did not consider the high pressures and temperatures present in geological CO_2 reservoirs (>10 MPa, >40 °C). Probably the first comprehensive study on high pressure and temperature physical adsorption of CO_2 on shale and clay samples was reported by Busch et al. ([2008]). It was shown that clay minerals adsorb large amounts of CO_2, with Ca-exchanged smectite adsorbing the largest amounts, followed by Na-exchanged smectite, illite and kaolinite, and negligible amounts of CO_2 adsorbed on chlorite. Clay samples were measured dry and equilibrated with laboratory humidity at CO_2 pressures of up to 20 MPa at a temperature of 50 °C. As for many microporous materials it was shown that the sorption capacity of clays is lowered in the presence of water. Comparable sorbed quantities as for smectite and illite clays were measured on a clay-rich shale sample from the Carnarvon Basin in Australia. Figure 1 shows a compilation of measured maximum excess CO_2 adsorption capacities versus specific surface areas (SSA), comparing different clays and shales (Amann et al. [2011]; Busch et al. [2008]; Gensterblum et al. [2009], [2010]; Jeon et al. [2014]). From this figure, it is evident that for clays, mudrocks, siltstones and activated carbon, excess

114

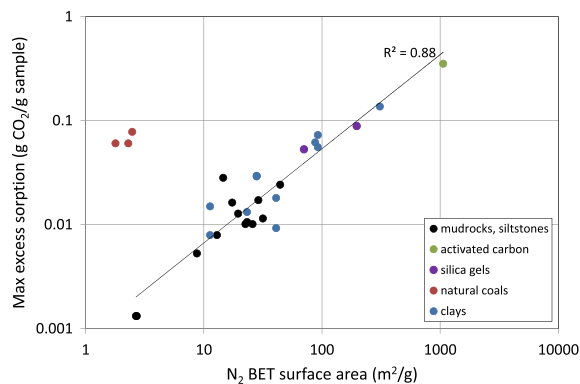Geomech. Geophys. Geo-energ. Geo-resour. (2016) 2:111–130

Fig. 1 Maximum CO_2 sorption capacity measured for different rocks and minerals at 45–50 °C and as a function of specific surface area determined using N_2 low pressure sorption. We observe a linear trend for the shale, clay and activated carbon samples, indicating that sorption is controlled by super micropores with pore sizes > ∼0.7 nm. Natural coals show higher adsorption capacities indicating that smaller pores, not covered by N_2 BET, significantly contribute to overall sorption capacity. Data on the clays, mudrocks and siltstones from Amann et al. (2011), Busch et al. (2008), Jeon et al. (2014); for the silica gels from Rother et al. (2013b), and for the natural coals and activated carbon from Gensterblum et al. (2009, 2010)

CO_2 sorption versus N_2 BET area follows a power law function ($R^2 = 0.83$), while the natural coals, included for comparison, consistently show higher adsorption capacities. Small micropores in coals and clays are too small for N_2 to enter, and hence do not contribute to the N_2-BET area. This suggests that sorption in the clays and mudrocks takes place in supermicropores (>0.7 nm, IUPAC terminology, Thommes et al. 2015), mesopores (2–50 nm) and macropores (>50 nm), while the coal samples seem to adsorb CO_2 in ultramicropores (<0.7 nm). Since large surface areas are typically associated with ultramicropores, the adsorption capacity in natural coals is significantly larger than in other materials (Figure 1).

An alternative explanation is that the excess sorption capacity of clays is generally not related to the large surface area of the interlayer space, but only to the mesopores between clay particles. While this may be true for nitrogen, accessibility of the interlayers of hydrated smectites to at least some fluids, including water and carbon dioxide, has been shown.

CO_2 sorption isotherms of clays and shales (but also other materials) consistently show that the excess sorption decreases after passing through a maximum, and sometimes even becomes negative at high fluid densities above the critical point. This maximum coincides with the steep increase of the CO_2 density

curve around the critical density of CO_2 (7.3 MPa). It is therefore lower than the pressure in reservoirs typically considered for CO_2 storage. Possible reasons for this have been discussed elsewhere; see for instance Rother et al. (2013a, b). Excess sorption describes the advantage of adsorbing gas (in this case CO_2) over storing it in the bulk phase. The difference between bulk density and pore density is the storage density in the accessible pore spaces. If the excess sorption is positive, the sorption phase is denser than the coexisting bulk fluid phase, and when excess sorption is negative it is more efficient to store CO_2 in the bulk pore volume. Consequently, when the excess sorption is zero, both densities are equal. Experimental issues can further complicate the pore storage efficiency assessment, as discussed in Siemons and Busch (2007) or Busch and Gensterblum (2011). Rother et al. (2013a) explicitly addressed the density of the sorbed phase. They report a combined excess sorption and neutron scattering study on Texas montmorillonite (STx-1) to investigate sorption amounts, interlayer swelling and sorbed phase density at temperatures of 35 and 50 °C and pressures up to 15 MPa. They found that at pressures below the critical CO_2 pressure ($P_c = 7.3$ MPa) the sorbed CO_2 density is higher than the gas density. At about 8–10 MPa equal bulk and sorbed phase densities of ∼300–400 kg/m^3 were observed. With further pressure increases, the bulk density becomes increasingly larger than the sorbed phase density, hence resulting in negative excess sorption. Similar observations have been made in earlier studies by the same authors on silica gels with defined pore geometries (Rother et al. 2013b). These findings partly confirm those by Busch et al. (2008) where a decreasing excess sorption trend was observed for pressures exceeding ∼8 MPa, but negative excess sorption (where the sorbed phase density is below bulk density) was not observed. Negative and near negative excess sorption of CO_2 on clays and shales was however reported by Busch et al. (2012). The origins of high-density interfacial fluid depletion are molecular, i.e., weakly attractive fluid solid interactions, causing fluid–solid interactions to be energetically preferred over fluid–solid interactions at low density, but fluid–fluid interactions are preferred at high density.

1.3 Sorptive swelling of clays with CO_2 exposure

As an extension of the sorption work, a series of studies report the swelling of different clay minerals

when charged with CO_2. Measurements were performed on smectite samples exchanged with different cations (K, Ca, Na) using X-ray diffraction (XRD) in an environmental chamber (Giesting et al. 2012a, b; Ilton et al. 2012; Schaef et al. 2012). All measurements on pure clay samples discussed below used standard clays provided by the Source Clays Repository, the Clay Minerals Society, hosted at the Department of Geology, University of Missouri, Columbia, MO, and described in detail by Costanzo and Guggenheim (2001). Swelling strain was measured at hydrostatic (pore pressure) conditions, i.e. no external load was applied. It was shown that swelling strain depends on the initial interlayer spacing. Dry, collapsed smectite, with an interlayer space of 0.95–1.0 nm, and non-expandable clays like illite do not show measurable swelling strain. This is different for smectite containing small amounts of water, i.e., when the hydration state is between discrete hydration states (0–1 W; 1–2 W, using the terminology of Ferrage et al. 2010). In this context the term 0 W is the dehydrated state with an interlayer spacing d_{001} of $\sim$0.95–1.0 nm, 1 W refers to one complete water layer ($d_{001} \sim$ 1.25 nm) and 2 W is indicative of two water ayers ($d_{001} \sim$ 1.5 nm). Smectite hydration states at

reservoir stress conditions are assumed to be between 0 and 2 W (Bird 1984). At 0 W no or little swelling strain is observed, but as hydration is increased towards 1 W, the swelling strain is increasing significantly. Close to the 1 W hydration state, swelling strain is returning to values close to zero strain. At higher hydration states, corresponding to very shallow burial depths, shrinkage of the interlayer spacing was observed (Schaef et al. 2012, Fig. 2), indicating water removal from the sample, possibly by water dissolving in CO_2.

Besides water content, swelling strain was also shown to depend on the interlayer cation. Giesting et al. (2012a, b) have demonstrated that the swelling strain from Na and K-exchanged samples is similar with a return to initial values at discrete water layers. This seems to be different for their Ca-exchanged equivalents that show higher swelling strains and only seem to return to initial values at a 2 W hydration state.

To transfer this information to subsurface conditions, it is essential to know the hydration state at different depths. As mentioned earlier, Bird (1984) calculated hydration states with burial depth from thermodynamic considerations, showing rough depth ranges where Ca
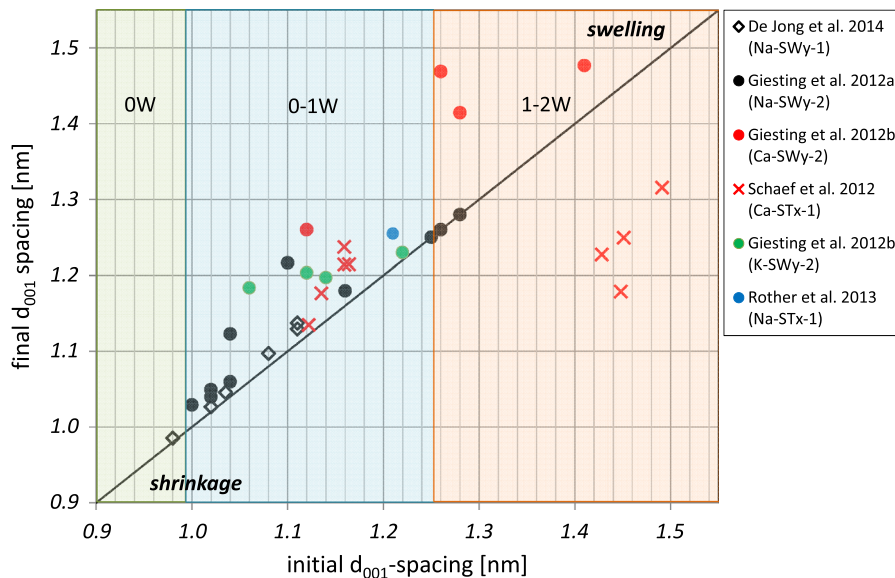

Fig. 2 Summary of maximum smectite interlayer spacing d_{001} after charging samples with CO_2. Hydration states (0, 1 W etc.) relate to interlayer water layers. These depend on the interlayer cation, on relative humidity, temperature and pressure (in this case only hydrostatic). Between the three hydration fields indicated in the figure are discrete states with almost all of the

clay minerals having the same hydration state (either 1 or 2 W). For all these measurements two different clays were used: Wyoming and Texas MMT, provided by the Clay Mineral Society and either used as provided or purified and cation exchanged. Data from de Jong et al. (2014), Giesting et al. (2012a, b), Rother et al. (2013a), Schaef et al. (2012)

or Na-exchanged smectites are rather in the 1 or 2 W hydration state. Unfortunately, Bird's calculations are on a basin scale, i.e., precise clay hydration states were not defined, and it remains unclear whether discrete or intermediate states are to be expected in a geologic reservoir. Different speculative models were developed for the mechanism of the observed swelling: Giesting et al. (2012b) discussed the configuration of CO_2 in the clay interlayer, suggesting the formation of a permanent carbonate species. This assumption was based on the observation that K and Ca-Wyoming smectite did not return to their respective original hydration states after a pressure cycle, i.e., a hysteresis remained. This effect became more pronounced with longer charging times. Permanent trapping of CO_2 in the interlayer of Na-exchanged smectite (Na-SWy-2), potentially as carbonates, was also indicated in the work by Hur et al. (2013) and Romanov (2013) from Fourier-transform infrared spectroscopy (FTIR) and X-ray diffraction data. However, CO_2 trapping in clays was not observed in a number of other studies: Krukowski et al. (2015) using FTIR on Na-exchanged (Na-STx-1), and Schaef et al. (2012) on Ca-exchanged (Ca-STx-1) Texas-montmorillonite using thermo gravimetric analysis, as well as Loring et al. (2012), also on the same Ca-exchanged samples using a variety of methods, such as magic angle spinning nuclear magnetic resonance spectroscopy and attenuated total reflection infrared spectroscopy. These measurements were performed at 50 °C and pressures up to 18 MPa.

Loring et al. (2014), using X-ray diffraction and IR spectroscopy at 50 °C and 9 MPa on Na-SWy-2, studied relative CO_2 uptake as a function of clay water content, and demonstrated a steep increase in CO_2 interlayer contents at low water saturations. This steep increase seems to correspond to a step in hydration from 0 to 1 W. With an increase in water content, this CO_2 concentration decreases and almost disappears when the clay interlayer distance moves to 2 W. This clearly demonstrates that the interlayer CO_2 uptake capacity is strongly related to the water content. It also confirms the observation that for Na-exchanged smectite (Giesting et al. 2012a) interlayer swelling occurs between 0 and 1 W only.

In a very recent study Schaef et al. (2015) demonstrated, using XRD, IR and quartz crystal microbalance (QCM) on variably hydrated Ca-SWy2, that the swelling depends on the relative amounts of H_2O and CO_2 in the interlayer. The interlayer space of dry

smectite increases sharply upon introduction of some water, and decreases again upon further hydration of the clay. These findings qualitatively confirm observations discussed above and demonstrate that clay swelling is feasible, when the interlayer distance is between 0 and 2 W. These states correspond to subsurface or reservoir conditions (e.g. Bird 1984), but shrinkage occurs for hydration states >2 W, i.e., at near-surface to surface conditions, likely due to the removal of water by dry scCO_2.

1.4 Swelling stresses induced by CO_2 sorption to clays

Zhang et al. (2014) reported the first datasets of experimentally determined swelling stresses for Na-exchanged Wyoming smectite (Na-SWy-2). The same samples have previously been used for the determination of swelling strain (e.g. de Jong et al. 2014; Giesting et al. 2012a). For different hydration states (dry, laboratory moisture equilibrated, wet), different effective stress conditions (representative for 1–2 km reservoir depth), and temperatures between 40 and 80 °C, isovolumetric swelling stresses in the range of 30–80 MPa were found. Control measurements using inert gases (Ar and He) or non-swelling clays (illite) showed significantly lower stresses. Using this range of values for swelling stresses, Wentinck and Busch (2014) calculated the shear capacity utilization (SCU) for different scenarios of reservoirs bound to a vertical fault or reservoir edge. This is schematically illustrated in a Mohr–Coulomb diagram in Fig. 3. The Mohr–Coulomb shear failure criterion is specified by the cohesion strength S_o and the friction angle ϕ. The
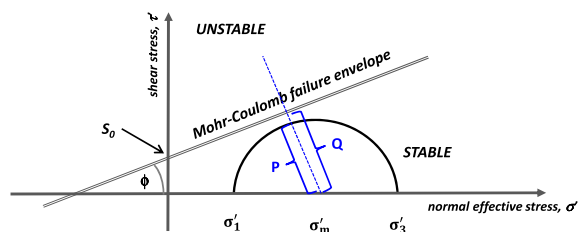

Fig. 3 Mohr–Coulomb diagram showing the principle parameters in Eq. 1 and the criteria for shear capacity utilisation (SCU). When the shear capacity of the caprock P utilises its full capacity Q, shear failure will occur. Shear failure can lead to a permeable pathway and therefore to fluid leakage from the reservoir

stress condition of a material point is represented by three Mohr circles of which the largest (between the effective principal stresses σ_1' and σ_3') is given in Fig. 3. A material point under consideration is perceived in an elastic state of deformation if the Mohr circle remains below the failure line, whereas the material is in shear failure if the circle touches the failure line (Fjær et al. 2008). The SCU normalizes the rock internal shear capacity τ in relation to its utilization τ_{max}, i.e. values <1 indicate stable, values >1 unstable conditions for the shear stress:

$$SCU = \frac{\tau}{\tau_{max}} = \frac{\sigma_1' - \sigma_3'}{2\left(\sigma_m' + S_0/\tan\phi\right)\sin\phi} \tag{1}$$

Here, σ_1' and σ_3' [Pa] are the maximum and the minimum effective principle stresses, respectively and σ_m [Pa] is the average of these stresses: $\sigma_m' = \frac{1}{2}\left(\sigma_1' + \sigma_3'\right)$.

Values for effective stresses depend on the pore pressure P_p, the swelling pressure S_p, and the lithostatic pressure. Wentinck and Busch (2014) have shown that for specific CO_2 storage scenarios, where the seal contains high amounts of swelling clays, the risk of shear failure is given for time scales in the order of 100s or 1000s of years. For shear failure to occur, a number of factors, like swelling clay content, effective stress conditions and related initial smectite interlayer spacing, diffusion coefficient controlling velocity of CO_2 penetrating the caprock, stress relaxation into the shale formation etc. have to be favourable for the development of significant swelling stresses. It remains difficult to predict if, in case of shear failure, a permeable pathway would develop.

This clearly is an important area for future research and critical parameters should be constrained, especially when it comes to fault behaviour and build-up and relaxation of stress following clay swelling.

1.5 Molecular dynamics studies

A limited number of molecular dynamics (MD) and grand canonical Monte–Carlo (MC) simulation studies aimed at the explanation of the experimental results presented above. In a combined MD and MC study, Botan et al. (2010) found for pressure and temperature conditions representative for CO_2 storage reservoirs, that at least one CO_2 molecule per clay unit

cell is capable of entering hydrated clay interlayers, hence qualitatively confirming the above experimental results. They did, however, not confirm the strain response upon CO_2 intercalation (neither swelling nor shrinkage). More recent MD studies using density functional theory demonstrate, that CO_2 is able to intercalate the clay mineral interlayer resulting in positive strain (Cygan et al. 2012; Myshakin et al. 2013, 2014; Spiering et al. 2014), and that the strain strength depends on the initial hydration state. These simulations were typically carried out at p, T representing supercritical CO_2 and therefore reservoir conditions ($P_c > 7.39$ MPa, $T_c > 31$ °C). It was shown that swelling increases with an increase in the number of water molecules, and with an increase in the number of CO_2 molecules per unit cell. It was also shown that different initial water/CO_2 molecular ratios lead to stable final states (0, 1 W, etc.). While this in general confirms the experimental observations, some discrepancies remain. In their systematic studies, Giesting et al. (2012a, b) showed that for the different cation-exchanged Wyoming smectite (SWy-2), swelling is most dominant just above the stable hydration states of 0, 1 W etc. This shows first of all that some interlayer water is needed to swell the sample (no swelling at 0 W), and that smectite at discrete hydration states (e.g. 1 W) do not exhibit major swelling. Between these defined states, the swelling strain increases initially, followed by a decrease with increasing hydration (cf. Figure 2). Spiering et al. (2014) argued that CO_2 acts as a "catalyst", promoting increased hydration of the interlayers. For the CO_2 case, this indicates that the swelling strain is larger compared to the non-CO_2 case at the same hydration state. Wentinck and Busch (2014) confirm this interpretation, and explain the swelling mechanism by the contribution of the entropy of mixing between H_2O and CO_2 to the chemical potential of the interlayer space. This contribution, albeit only in the 100 s of Joule/mole-range, is large at low water content in the interlayer. However, it is critical as it results in cation hydration at lower relative humidity, i.e., clay hydration, compared to the non-CO_2 case. This hypothesis is in agreement with Loring et al. (2014) who showed an initial steep increase in CO_2 interlayer concentrations with increasing water contents in the range between 0 and 1 W, followed by a decrease towards higher hydration states.

2 Potential CO$_2$ leakage scenarios associated with clay swelling

In the following section we discuss implication of the CO$_2$/clay interaction on CO$_2$ trapping in the reservoir, CO$_2$ leakage along wellbores, faults and fractures, or through the capillary network of the caprock. We begin with an assessment of where these mechanisms might be of relevance, and then discuss them separately. We show that sorption and swelling of clays need to be considered in reservoir modelling, especially in the potential for CO$_2$ trapping and geomechanical effects around wellbores and faults. The potential locations of interest are graphically illustrated in Fig. 4: Scenarios 2–5 are direct leakage scenarios, while scenario 1 relates to clay minerals in the reservoir, contributing to storage capacity. For all scenarios, all clay minerals are assumed to take up (adsorb) CO$_2$, but only smectite will exert a swelling force onto the surrounding rocks. Mechanisms and constraints are studied to provide insights on the possible benefits and risks of clay sorption and swelling.

2.1 CO$_2$ sorption on clay mineral surfaces in the reservoir

Gas adsorption on mesoporous materials is a well-known phenomenon in general and it is understood that the physical sorption capacity is proportional to the accessible SSA. SSA of typical reservoir rocks can vary by orders of magnitude. SSA of sand (2–0.05 mm) and silt size particles (0.05–0.002 mm), calculated assuming perfect spheres, vary between 0.001–0.04 and 0.04–1.1 m^2 g^{-1}, respectively. In contrast, clays exhibit a much larger surface area. Commonly reported values from N$_2$-BET are 5–15 m^2 g^{-1} for kaolinite, 25–40 m^2 g^{-1} for illite, 5–15 m^2 g^{-1} for chlorite and 80–120 m^2 g^{-1} for smectite (Meunier, 2005), while the total smectite surface areas including the interlayer space can reach values of up to several hundred m^{2}g^{-1}. As different analytical methods often give different SSA values, particularly for smectites, it seems that the area strongly depends on the method used and the respective measuring conditions using different gases, temperatures and pressures. Nitrogen physisorption, the most commonly used analysis for surface area determination, is most meaningful for supermicropores, mesopores and smaller macropores (Bertier et al. in press). Areas from CO$_2$ physisorption at 273 K yield

Fig. 4 Different scenarios of CO$_2$ interacting with clay minerals ▶ leading to sorption (for all clays) and swelling (only smectite). *Scenario 1* CO$_2$ sorption by clays dispersed in the reservoir. *Scenario 2* Reservoir-seal interface with CO$_2$ diffusing into the clay-rich seal and water diffusing from the seal towards the CO$_2$-filled reservoir. This potentially leads to gas uptake and swelling and therefore to mechanical stressing of the interface. *Scenario 3* Fault surfaces and damage zones getting in contact with CO$_2$ or CO$_2$-rich fluids might take up CO$_2$, especially when in contact with clay smear. This might change shear potential by lowering normal stress but also by an alteration of mechanical rock properties. *Scenario 4* CO$_2$ or CO$_2$-rich fluids entering a fracture system might interact with fracture surfaces, lower effective stress by creating swelling stress and either close fractures or contribute to fracture propagation. *Scenario 5* CO$_2$ potentially leaking along a wellbore-seal interface might swell the shale caprock and induce swelling stresses that could lead to the formation of microfractures or to the closure of the annulus between cement and caprock

considerably higher surface area values for smectites (Thomas and Bohor 1968), i.e. CO$_2$ provides information on ultramicropores but limited information on larger pores. Nevertheless, the SSA of clays are several orders of magnitude higher than those of quartz, feldspar and most other common reservoir rock minerals, and even a few percent of clay will increase the bulk rock surface area significantly.

A resulting key question is whether CO$_2$ sorption to clays offers a significant trapping potential. Adequate storage reservoirs have high porosity and permeability, and consequently tend to contain only small amounts of clay. Clay mineral contents of CO$_2$ storage reservoirs reported in literature are 3 % for Sleipner, Norway (Audigane et al. 2005), 7 % for Frio, USA (Xu et al. 2010), 8 % for Ketzin, Germany (Foerster et al. 2010), and 8 % for Goldeneye, UK (Hangx et al. 2013; Snippe et al. 2012). These numbers will be used to calculate the significance of CO$_2$ trapping by sorption for a simplified case. Considering a reservoir rock of idealised mineralogical composition (quartz = 90 %, clays = 10 %) and a porosity of 20 %, we calculate trapping mechanisms assuming equilibrium conditions (Table 1). Equilibrium implies complete saturation of brine with CO$_2$ and complete occupation of the clay sorption sites with CO$_2$. We use Duan and Sun (2003) for the calculation of CO$_2$ dissolution in brine at various salt contents, and Span and Wagner (1996) to calculate CO$_2$ densities at varying p–T-conditions. The variation of the sorption capacity with depth is calculated following the approach used by Gensterblum et al.
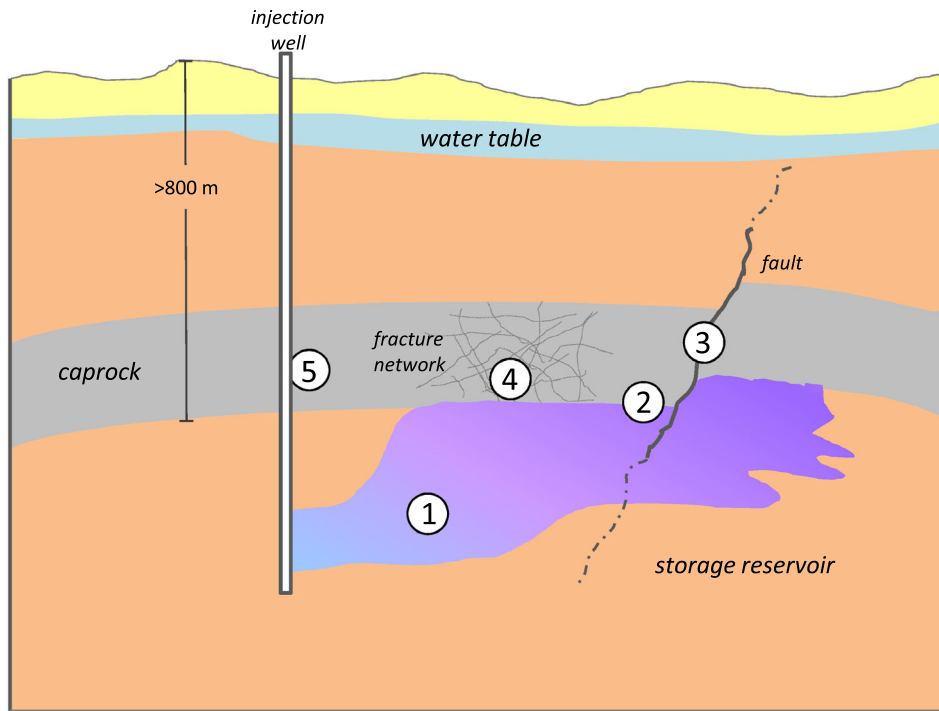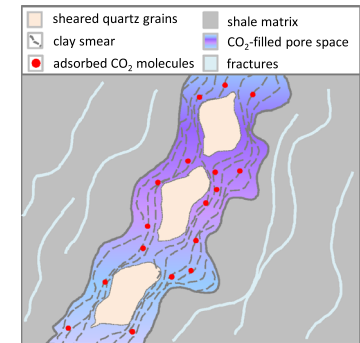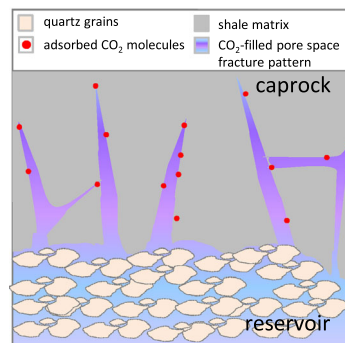
120
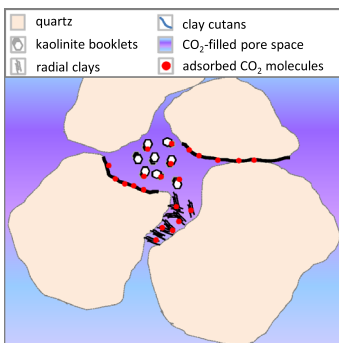
Geomech. Geophys. Geo-energ. Geo-resour. (2016) 2:111–130
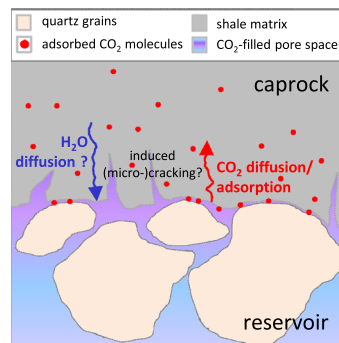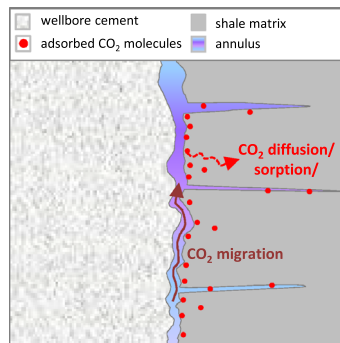
Table 1 Reservoir parameters and mineralogy of the hypothetical reservoir used in this calculation

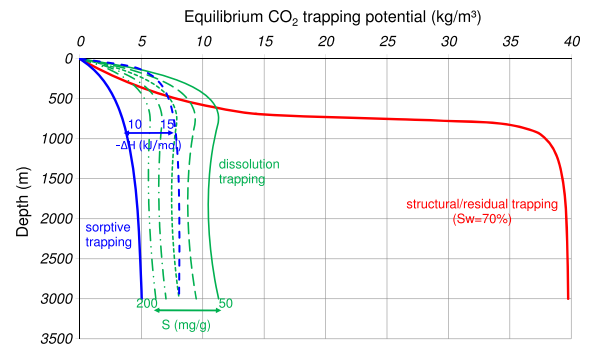|	Unit	Value
Reservoir parameters		
Geothermal gradient (ϑ)	K m^{-1}	0.03
Hydrostatic gradient (γ)	MPa m^{-1}	0.01
Porosity (ϕ)	–	0.20
Water saturation (S_w)	–	0.70
Mineralogy		
Quartz	g g^{-1}	0.90
Clay/Mica	g g^{-1}	0.10
Langmuir parameters for clay sorption		
Langmuir pressure (V_L)	mmol g^{-1}	1
Langmuir pressure (P_L)	MPa	6

Fig. 5 Equilibrium CO_2 trapping potential of hypothetical sandstone reservoir. All values were calculated assuming a geothermal gradient of 0.03 K/m and a hydrostatic gradient of 0.01 MPa/m. CO_2 dissolution in formation brine and CO_2 densities were calculated according to Duan and Sun (2003) and Span and Wagner (1996), respectively. For sorptive trapping we assumed a Langmuir volume of 1 mmol/g and heats of adsorption between −10 and −15 kJ/mol following the approach of Gensterblum et al. (2014)

(2014). This approach considers the Langmuir equation as a starting point:

$$n(p) = n_\infty \left(\frac{P}{P_L + p} \right), \tag{2}$$

where n_∞ is the Langmuir volume, P_L the Langmuir pressure, and $n(p)$ is the sorbed amount at a given pressure p under isothermal conditions. Langmuir volume (maximum number of sorption sites) is independent of temperature, hence only the Langmuir pressure depends on the sorption enthalpy, and can be calculated according to:

$$P_L(T) = P_0 \exp\left(\frac{-\Delta H_{KL}}{RT} \right) \tag{3}$$

where P_0 is a pre-exponential factor (described in Gensterblum et al. 2014), R universal gas constant, T temperature and $-\Delta H_{KL}$ the sorption enthalpy. Combining Eqs. 2 and 3 and integrating with respect to depth, yields the sorption capacity as a function of depth z:

$$n(z) = n_\infty \left(\frac{\gamma \cdot z}{P_0 \exp\left(\dfrac{-\Delta H_{KL}}{R(\vartheta \cdot z + T_0)} \right) + \gamma \cdot z} \right) \tag{4}$$

with γ being the hydrostatic pressure gradient, ϑ the geothermal gradient, and T_0 surface temperature.

In Fig. 5, residual/structural, dissolution and sorptive trapping are shown normalized to 1 m^3 of rock. As expected, residual/structural trapping are dominant, assuming a residual water saturation of 70 %, which is comparable to values reported by Al Mansoori et al. (2010); Iglauer et al. (2009). Dissolution trapping decreases with an increase in salinity (between 0 and 200 mg/g NaCl). Sorptive trapping is close to or slightly lower than dissolution trapping, and depends strongly on the sorption enthalpy, which varies with clay mineral type and water content in the smectite interlayer. Here we assumed rather low (conservative) sorption enthalpies between −10 and −15 kJ/mol, as opposed to roughly twice as high values observed for other microporous geomaterials like coal (e.g. Gensterblum et al. 2014).

Sorption and structural trapping are complementary processes, though they do take place in the same pore spaces. In Fig. 5, sorption capacity is calculated in absolute amounts. Note that, depending on its physical characteristics (density and volume), a sorbed layer will fill a certain volume of the pore space. Consequently, the pore space accessible to bulk CO_2 is reduced. As long as the sorbed phase density has a higher value compared to the bulk density, any storage capacity will benefit from this trapping mechanism, since some of the injected CO_2 will not contribute to pressure-buildup and increase the overall storage capacity. However, it was shown in several studies

(e.g. Busch et al. 2012; Rother et al. 2013a) using manometric and gravimetric sorption devices, and neutron diffraction techniques, that the excess sorption capacity can become negative at pressures exceeding ~ 10 MPa. This means that the sorbed layer has an average density smaller than bulk CO_2, and therefore the same amount of fluid in the sorbed layer will occupy a larger volume as compared to the bulk. A practical consequence is that injection of the same quantity of CO_2 will result in higher pressures in a reservoir with negative excess sorption capacity.

2.2 CO_2/clay mineral interaction at the reservoir-seal interface

Following the injection of CO_2 into storage reservoirs the CO_2 is buoyant because its density is lower compared to formation waters. Depending on this density difference, pressure gradients and permeability, a CO_2 plume will gradually rise towards the reservoir/seal interface, and progressively increase in water saturation. Depending on injection design and reservoir geometry, a continuous CO_2 column with column height h will establish underneath the seal. This column height exerts a certain differential pressure Δp across the interface, that is higher than the hydrostatic pressure in the aquifer. For depleted reservoirs this pressure might initially be lower than original hydrostatic, but could exceed hydrostatic pressure at some point after reservoir re-pressurisation. When this pressure exceeds the capillary entry pressure of the seal, CO_2 will enter the capillary network of the mudrock, resulting in leakage. This pressure is termed capillary entry pressure P_c, and details were provided earlier (e.g. Busch and Amann-Hildenbrand 2013). The column height h needed to initiate this process is given by:

$$h = \frac{P_c}{\left(\rho_{brine} - \rho_{CO_2}\right) \cdot g} \tag{5}$$

where ρ_{brine} and ρ_{CO2} are the brine and CO_2 densities under subsurface conditions, and g is the acceleration due to gravity.

The capillary entry pressure P_c is defined as the pressure difference Δp across the reservoir/seal interface, and depends on wettability and interfacial tension between the two phases: water and CO_2, and is expressed following the Laplace equation:

$$\Delta p = P_c = \frac{2\gamma \cdot \cos(\theta)}{r} \tag{6}$$

where γ is the interfacial tension between CO_2 and water, θ is the contact angle, and r the radius of the largest capillary in contact with CO_2 in the seal. Several correlations for P_c in relation to e.g. permeability are summarized in Busch and Amann-Hildenbrand (2013), where it was found that P_c is difficult to predict for mudrocks having permeabilities $<10^{-18}$ m^2.

Assuming that reservoir management is such that buoyancy does not exceed the seal entry pressure, i.e., no viscous flow occurs through the capillary seals, diffusion is the dominant transport mechanism (see Fig. 4, case 2). Diffusion is driven by concentration gradients between the bottom (the reservoir/caprock interface) and the top of a shale package. Initially, the CO_2 concentration C_2 at the top of the seal can be considered zero. At the bottom we need to distinguish between CO_2 dissolved in brine C_{diss} and CO_2 adsorbed C_{ads} to mineral surfaces or organic material. Significant amounts of organic material only occur in specific cases, such as gas shale plays and in our case we assume this to be absent. To demonstrate diffusion through a shale package, Fig. 6 shows the results of a modeling attempt as described in detail in Busch et al. (2008), Krooss et al. (1992) which is based on Fick's law of diffusion:
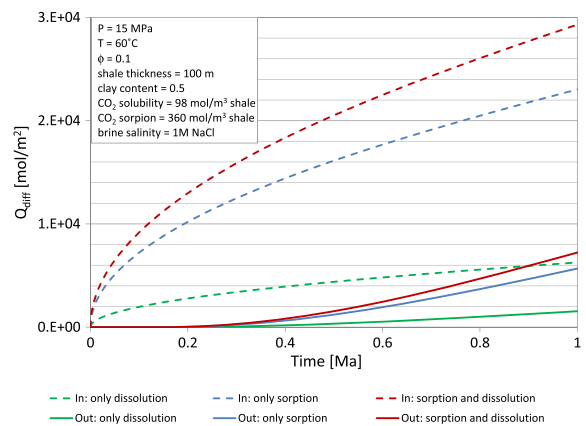

Fig. 6 Diffusive CO_2 transport through a shale of 100 m thickness. D_{eff} is assumed to be 10^{-10} m^2/s and sorption capacities have been assumed based on Busch et al. (2008), CO_2 solubility in brine is calculated from Duan and Sun (2003). The diffusion model is proposed by Krooss et al. (1992) and was applied to calculate diffusional fluxes versus time

$$J_D = -D_{eff}\nabla C_{bulk} \tag{7}$$

$$C_{bulk} = C_1 - C_2 = (C_{diss} + C_{ads}) - C_2 \tag{7a}$$

The rate at which CO_2 is diffusing through the shale package is determined by the effective diffusion coefficient D_{eff} (we assume a value of 10^{-10} m²/s which is at the higher end of published values) and the CO_2 concentration at the caprock/reservoir interface (C_1 in mol/m²). For calculating C_1 we assume a reservoir pressure and temperature of 20 MPa and 353 K, corresponding to a depth of about 2000 m. The thickness of the shale is 100 m with porosities of 10 % and clay contents of 50 %. The CO_2 sorption capacity of the shale C_{ads} is assumed to be 360 mol/m³, based on the clay content and rather conservative excess sorption values of 0.3 mmol/g (e.g. Busch et al. 2008). This value is taken from excess sorption measurements but used here as absolute sorption, not considering the contributions from pore filling with bulk fluid to storage capacity. Our reasoning is that absolute adsorption is always higher than excess sorption, and excess can therefore be considered as a lower boundary for storage capacity at any pressure (see Busch and Gensterblum 2011 for a detailed description). Carbon dioxide solubility C_{diss} of 98 mol/m³ is calculated from Duan and Sun (2003), assuming a 1 molar NaCl brine solution. Figure 7 shows the diffusive fluxes into and out of the shale package after a vertical distance of 100 m. The difference between inflow and outflow is
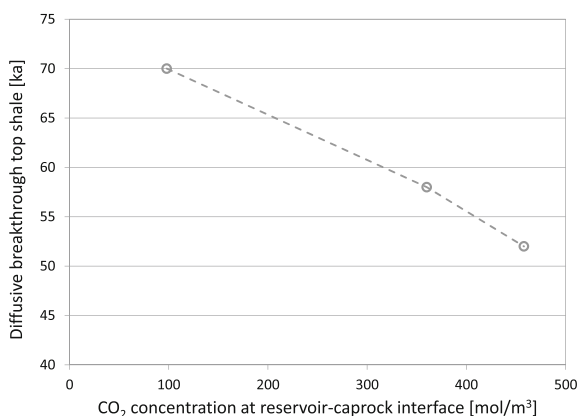
the "CO_2 storage capacity" of the shale, here interpreted as C_1. Figure 7 shows this C_1 value versus the estimated time required for CO_2 to break through at the top boundary of the shale. It becomes apparent that the higher the C_1 value (or the concentration gradient) the more rapid breakthrough occurs, while the time window for the three cases analysed here do not differ significantly from a geological perspective and vary between ∼50,000 and ∼70,000 years. At the time of breakthrough, ca. 2.9 kg CO_2/m³ has been stored in the shale package by sorption (2.24 kg CO_2/m³) or dissolution (0.66 kg CO_2/m³). One limitation of this calculation is that a possible change in CO_2 concentration at the lower shale boundary is not considered, which may occur over time. Such changes could be caused by changes in reservoir pressure and/or CO_2 concentration at the interface, which likely increase during injection and decrease thereafter. Such changes will, however, rather occur over geological than engineering time scales, and will have little impact on storage containment or capacity.

In summary, CO_2 sorption on clay minerals in shale formations will increase flux rates after CO_2 breakthrough, while times scales for breakthrough are still far above the critical time scale of 10,000 years requested by most regulators. At the same time, depending on the details of the CO_2 concentration gradients across the seal, significant amounts of CO_2 will be temporarily immobilized, which contributes to storage safety and to a reduction in reservoir pressure.

2.3 Implications for shear failure

The likelihood for the reactivation of pre-existing faults predominantly depends on current stress states. Faults are critically stressed when the state of stress equals the Coulomb faulting criterion. This mainly depends on fault orientation with respect to the direction of maximum stress (Barton et al. 1995). Samuelson and Spiers (2012) provided experimental evidence that the fault friction properties are not affected significantly by CO_2, i.e., only critically stressed faults are able to slip when storing CO_2. It was also shown, that only mechanically active faults can become hydraulically active or permeable (Townend and Zoback 2000), and the risk of loss of containment exists only for permeable faults.

Wentinck and Busch (2014) performed a numerical study of the potential for shear type failure in a smectite

Fig. 7 Plot showing the concentration of CO_2 at the reservoir/caprock interface (C_1), determined by CO_2 sorption and solubility at equilibrium conditions versus the time required to travel through a 100 m thick shale package with D_{eff} of 10^{-10} m²/s

rich caprock around a fault offset. The smectite content was considered to be 30 %, which is typical for many North Sea regional caprocks (Pearson 1990). In the study, transport was modeled by aqueous diffusion only, at a rate of $D_{eff} \sim 10^{-10}$ m^{2}s^{-1}, and clay sorption, swelling strain, and swelling stress data from literature sources summarized earlier in this paper were used. The reservoir conditions studied were 20 MPa and 353 K. It was shown that the swelling pressure affects the effective pressure such that the shear capacity (cf. Eq. 1) exceeds a value of 1, potentially resulting in shear-type failure. This process was modeled as a function of a diffusional front migrating through the caprock. Migration by diffusion was estimated to be on the order of mm or cm per year. When the diffusional front has migrated far enough into the caprock (on the order of meters—after 100's to 1000's of years), the shear capacity utilisation of the caprock can be exceeded. This is because clay swelling results in significant stress build-up, affecting shear stresses, and eventually leading to mechanical failure. In the case that this mechanical shear failure creates a permeable path, loss of containment would be the consequence.

Many relevant aspects for the estimation of shear-type failure due to CO$_2$/clay interaction are still not well understood. This is the case for the exact swelling strain and swelling stress that will evolve and largely depends on the fluid composition, layer charge, and cation identity inside the smectite interlayer spaces (see discussion above). Although Bird (1984) has estimated the hydration state of different cation-exchanged smectites for different burial depths, calculations are rather rough, i.e. on the basin scale but not on the reservoir scale. Hence, clay fractions could be in stable or discrete hydration states, and pressure build-up could therefore be non-existent or limited. Furthermore, it remains largely unknown as to what extent relatively immature, smectite-rich mudrocks will relax such swelling pressure by inherent plasticity (or ductile creep), especially over time scales needed to establish a significant pressure profile. In addition, the caprock thickness needed to create high permeability cracks or to reactivate fault remains uncertain. Even in the case fault permeability would develop, limited information is available on potential flow rates.

In summary, there is a chance of clay swelling leading to significant swelling stresses, causing shear-type failure and potentially loss of containment along a permeable fault. However, many relevant parameters need to be quantified with a reasonable level of confidence on a case by case basis in order to determine the actual risk of loss of containment.

2.4 CO$_2$ in natural or induced fractures

Fractures are important pathways for fluid migration, both within a reservoir and across a seal unit (Carey et al. 2015). Even if such pathways are present, either naturally or induced they can be impermeable due to self-sealing. The step from open to closed fractures is usually assumed to be in line with the ductile to brittle transition. This transition again is considered to be related to the clay content of the clay-rich caprock and a recent study postulated this content to be $\sim 1/3$ (Bourg 2015). When CO$_2$ enters fractures in the caprock or within fault damage zones, either by aqueous diffusion or as a viscous phase, it will adsorb to clay minerals at the fracture surfaces. These clays can be aligned at different angles to the fracture surface, depending on how the fractures were generated. Neglecting any chemical effects (see Fitts and Peters 2013 for details) clay swelling results in decreasing fracture apertures for clay particles oriented parallel to the fracture surface,. Assuming a certain swelling strain for each of the two surfaces within a fracture, a simple relation between fracture aperture a [m] and fracture transmissivity k_f [m^2] can be derived:

$$k_f = \frac{a^2}{12}. \tag{8}$$

As an example, a fracture permeability decrease by 36 % is calculated assuming 10 % swelling strain as demonstrated for pure smectite (Giesting et al. 2012a, b), or ~ 20 % assuming 5 % swelling strain, which might be more realistic for shales of mixed mineralogy.

When considering a formation with a spacing b [m] between the fractures, Eq. 7 can be extended for sheet (Eq. 8), match-stick (Eq. 9) or even cubic structures (Eq. 10), with the permeability decrease being the same as for the single fracture described in Eq. 7:

$$k_{f\_sheets} = \frac{a^2}{12}\phi_f^3 \qquad (9)$$

$$k_{f\_match-sticks} = \frac{w^2}{96}\phi_f^3 \qquad (10)$$

$$k_{f\_cubes} = \frac{a^2}{162}\phi_f^3 \qquad (11)$$

Here $\Phi_f = a/b$ is the fracture porosity (see Reiss 1980 for details).

2.5 Leakage along the wellbore-seal interface

2.5.1 Formation dehydration around a wellbore

Wells might have either been used for production that were drilled within different decades in the past or might be drilled specifically for injecting or monitoring CO_2, using latest drilling and completion technologies. For example, a former production well might have experienced higher temperatures from produced fluid as compared to the injected CO_2. This has consequences on contraction and expansion of the cement sheath and the surrounding host rock, and a small annulus of micrometer diameter can form between cement and host rock (e.g. Bois et al. 2009; Gasda et al. 2004; Loizzo et al. 2011). Although such an annulus is unlikely to form in case of a competent cement job, it cannot be ruled out. If pressure gradients are formed inside the well, which is likely during the injection period, significant cooling of the well caused by the Joule–Thomson effect may occur, especially when injecting into depleted reservoirs with high pressure gradients. This wellbore annulus can develop apertures in the order of 10–300 μm (Bachu and Bennion 2009), especially when cold CO_2 is injected. Thermal shrink-age of the cement and casing steel as well as surrounding shale can occur. The thermal coefficients are 9×10^{-6} K^{-1} for Portland cement (Barlet-Gouedard et al. 2009), and between $\sim 10^{-4}$ K^{-1} to 10^{-5} K^{-1} for shale, depending on orientation, water saturation and shale type and characteristics (Moha-jerani et al. 2012, 2014; Monfared et al. 2011; Wang et al. 1996). Especially quartz-rich formations are sensitive to thermal cracking, which is due to the large differences in the thermal expansion coefficient of quartz in comparison to other minerals such as clays. Another scenario is the shrinkage of montmorillonite in clay rich formations around the wellbore with hot fluid production. This is even more the case if it has taken place over long periods of time (e.g. Dusseault 2011) or an increased water uptake capacity in swelling clays when cold fluids (CO_2) are injected. Shrinkage of swelling clays may lead to local and temporal pore pressure changes due to redistributions of the void space and mineral volume in a pore. This is the case when the pressure pulses are not transported to the far field. As a consequence of thermal shrinkage due to cooling some CO_2 might leak along an annulus that has potentially formed and extends to the surface, or into overlying, shallower strata. In the case of dry CO_2 leakage, shale desiccation is reasonable to assume, which might have implications on CO_2 transport and sorption in the host rock. In this case, cracks could form, allowing CO_2 to enter the formation laterally at increased flow rates, changing from pure aqueous diffusion to viscous flow. The rates of diffusive water flux from the formation towards the annulus against the water uptake capacity of CO_2 leaking along the annulus to determine the dominant transport mechanism (see Fig. 4, case 5 for an illustration). We here consider a scenario where the CO_2 density at 2000 m depth (20 MPa, 80 °C) is ~ 637 kg/m^3 (Span and Wagner 1996). Under these p,T conditions, CO_2 dissolves ~ 1 mol ‰ H_2O (Spycher et al. 2003). Other important parameters are the diffusion coefficient (10^{-10} to 10^{-12} m^2/s, e.g. Busch et al. 2008; Schlömer and Krooss 1997, 2004), concentration gradient for diffusing species, the contact area between annulus and shale formation (or the annulus length), and the annulus aperture itself (10–300 μm). The pressure gradient Δp is 20 MPa in the case of a direct connection to the surface, and assuming no overpressure from injected CO_2 (which is likely). The gradient is smaller when CO_2 is leaking into permeable reservoirs at shallower depth. In order to perform a rough mass balance calculation between water in-flow rates compared to uptake rates by the CO_2, we use Fick's Law to calculate diffusional fluxes of water to the annulus (Eq. 7). If we assume the effective diffusion coefficient D_{eff} to be 1.0×10^{-10} m^2 s^{-1}, the concentration difference Δc to be 6.1 mmol.mol^{-1} (~ 100 mol H_2O/m^3 CO_2, e.g. Spy-cher et al. 2003), and the distance Δx to be 0.1 m (for which it takes the CO_2 about 3.2 years to diffuse to—so well within the timescale of a CO_2 storage operation), we obtain flux rates of ~ 0.1 μmol m^{-2} s^{-1} from the formation to the wellbore annulus. Assuming an

annulus diameter of 0.2 m and a caprock thickness of 100 m, we calculate diffusional flux rates of ~ 6 μmol H_2O per second from the host rock to the wellbore.

In contrast, if we consider Newtonian flow of leaking CO_2 along the wellbore annulus, we obtain:

$$Q_{CO2} = -\frac{\pi}{12\mu}\frac{\Delta p_f}{\Delta L}\left(r_2^2 - r_1^2\right)(r_2 - r_1)^2, \qquad (12)$$

with Q being the flow rate (mol s^{-1}), μ the viscosity (Pa s), r_2 and r_1 the outer and inner annulus radii, respectively, Δp_f the pressure gradient along the wellbore (MPa), and ΔL (m) the length of the leaking wellbore, we can calculate the CO_2 uptake capacity for water flowing along the annulus and being transported to the surface. Assuming an outer diameter of the annulus of 0.2 m, and an annulus slit of 30 μm, we calculate that ~ 1 mmol CO_2 s^{-1} is leaking along the well. This CO_2 can take up ~ 1 μmol H_2O, corresponding to rates of ~ 10 μmol s^{-1}. This rate is close to the influx rate of water from the host rock (~ 6 μmol s^{-1}), hence shale dehydration is realistic. Parameters that could differ on the order of magnitude scale are the diffusion coefficient (typically ranges between 10^{-10} and 10^{-12} m^2 s^{-1}, Schlömer and Krooss 2004), and annulus aperture (ranges between 10 and 300 μm). Both a decrease in diffusion coefficient and increase in the annulus radius between cement and host rock would result in accelerating shale desiccation, since less water is transported to the well, and more water would be transported to upper levels, respectively.

These calculations suggest that shale desiccation in a well having an annulus between cement and rock is realistic, while the extent of which depends on a few parameters that need to be obtained in order to get quantitative results. Progressive desiccation might result in increased caprock accessibility for CO_2, and therefore an increased potential for sorption and swelling, but also for shrinkage. If the shale contains large amounts of swelling clays, and dry CO_2 is able to remove some or all of the interlayer water, desiccation cracks are likely to form, that will even further increase communication between shale and wellbore. This, however, is only likely in the case that the leaking CO_2 has a continuous communication to either shallow aquifer or the surface. When CO_2 in the annulus becomes stagnant, saturation with formation

water can be expected to happen quickly, resulting in a limited shale desiccation.

2.5.2 CO₂ sorption/swelling of clays around wellbore annulus

What can be expected from sorption/swelling of clay minerals around potentially leaking well bores? Considering mature shales without swelling clays no CO_2-induced clay swelling is assumed, and some of the leaking CO_2 will simply be adsorbed to clay minerals like illite or kaolinite. When the host rock consists of significant amounts of swelling clays, higher amounts of CO_2 will adsorb, and swelling (volumetric expansion) and the exertion of an anisotropic swelling stress acting on the formation, demonstrated in laboratory and modeling studies discussed above (Giesting et al. 2012a; Wentinck and Busch 2014; Zhang et al. 2014), will occur. In principle, the effect on well bore stability has been studied earlier: When water-based drilling mud with a salinity that differs in composition and concentration from the fluids in the mudrocks is used, a certain hydration (swelling) force might be exerted on the formation, leading to formation break outs (e.g. van Oort 2003). The severity of this effect depends on rock mineralogy (e.g. amount of smectite), ionic diffusion coefficient from the mud into the formation, type of solutes in the drilling mud, transportation of pressure pulses into the formation, but also the cementation factor (that keeps the rock intact). Although the occurrence of well stability issues is rather unrealistic since the well is cased when CO_2 is entering the annulus, other damaging effects are more likely. In case of mudrock swelling, volumetric expansion and the following fluid pressure effects become important. As discussed in van Oort (2003), swelling pressure, as defined by Eq. 13, will lower effective stress (σ_{eff}), and might shift the rock from a stable towards an unstable state in the classical Mohr–Coulomb diagram. This is schematically shown in Fig. 8, and mainly depends on the swelling pressure (p_s). Theoretically, clay mineral swelling could cause a pore pressure increase by reducing porosity, however, as already pointed out by van Oort (2003), the pressure front moves through shales much faster than a potential ionic diffusion front. Therefore, applying Therzaghis principle, the stress relation can be expressed as:
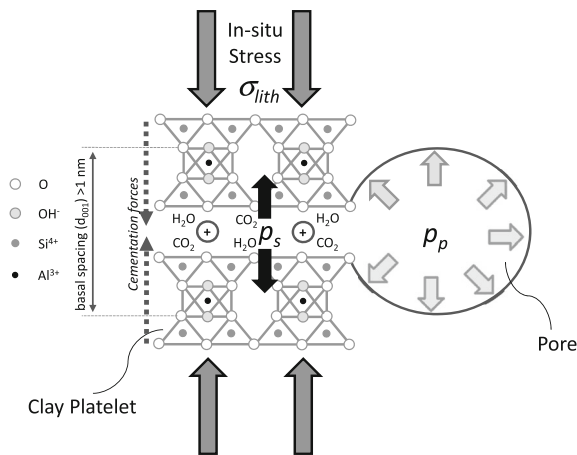
Fig. 8 Schematic illustration of different forces acting on and generated by clay platelets, connected to a pore (re-drawn from van Oort 2003). The interlayer distance between the TOT smectite sheets is considered to change due to changes in chemical potential which is achieved when changing H_2O, CO_2 or cation (marked as a *plus* sign) concentrations or composition. A swelling pressure is generated when CO_2 is introduced as shown above. This swelling pressure adds to the pore pressure and might lower the effective stress acting on the shale material. Contrary, in situ *vertical* and *horizontal stresses* are acting on the shale in addition to cementation forces

$$\sigma_{eff} = \sigma_{lith} - p_p - p_s \qquad (13)$$

with σ_{lith} the lithostatic stress, and p_p the fluid pressure van Oort (2003) describe a cementation force, that is addint to the lithology stress, which is however, not accounted for in Eq. 13. Cementation forces can be described as chemical contact points between mineral grains, and could, in theory, be related to the sample frictional or cohesive forces. Cementation forces might therefore be lower for weak mudrock, and higher for cemented sandstones or deeply buried, mature shales.

3 CO₂ storage in (depleted) gas shale reservoirs

A number of articles discuss the possibility of storing CO_2 in depleted gas shale reservoirs, or to use CO_2 for enhancing shale gas production (e.g. Edwards et al. 2015; Khosrokhavar et al. 2014; Li and Elsworth 2014; Tao and Clarens 2013; Godec et al. 2013; Kang et al. 2010; Liu et al. 2013; Nuttall et al. 2009). These concepts are similar to CO_2 enhanced coalbed methane recovery (CO₂-ECBM), which were tested and discussed in the literature mainly in the 1990's and

2000's (e.g. Reeves 2001; van Bergen et al. 2006). The enhanced methane recovery process in shales is different from the volumetric displacement of methane in coal reservoirs, in which a higher affinity for CO_2 compared to CH_4 drives the methane recovery and results in high amounts of CO_2 stored in the rock. Challenges are the commercial availability of CO_2, kinetics of CO_2/CH_4 exchange and swelling of the coal matrix due to CO_2 sorption that will significantly reduce permeability.

Applying these concepts to shale gas reservoirs, the potential benefits remain largely unchanged, while the drawbacks and complications will be amplified:

As for coal, the CO_2 sorption capacity of clays seems to be higher compared to CH_4 (e.g. Chareonsuppanimit et al. 2012; Weniger et al. 2010), but the overall sorptive uptake significantly lower. This is because high sorption capacities in coal are linked to its high organic matter content, which is much lower in shale. Replacing CH_4 by CO_2 in shale is largely a diffusion-driven process. Fracture spacing in shale determines matrix block sizes, with larger fracture spacing resulting in lower CO_2 accessibility. Permeability in coal is orders of magnitude higher (mDarcy) compared to shales (μ to nDarcy), indicating a much more narrow cleat network in coal compared to fracture networks in shale, or larger cleat compared to fracture apertures. Large fracture spacings require long diffusive travel times, hence slow exchange rates for the sorbed gas.

Coal shrinks with CH_4 desorption and swells with CO_2 adsorption. Shrinkage and swelling are directly related to the amounts of sorbed gas. Because sorption capacity for CO_2 is larger than for CH_4, coal swelling is more pronounced with CO_2 adsorption, and leads to permeability reductions by orders of magnitude. Shale swelling with CO_2 sorption has not been verified, but is plausible (as discussed above), and might cause similar issues. Gas shale reservoirs typically require reservoir temperatures that passed the gas window at temperatures around or higher than 100 °C. This might have caused a significant or even complete transformation of swelling clays to non-swelling species, as has been discussed above.

In summary, we consider the utilisation of shale reservoirs or shale formations for storing CO_2 or for an enhancement of natural gas recovery challenging and not well understood. A technology that did not reach a commercial stage when applied to coal beds seems to

not benefit from lower permeabilities, lower sorption capacities and generally larger depths in shale gas formations. For sure, more research is needed to better understand the interplay between all these parameters.

4 Conclusions

We discussed the implications of CO_2 clay mineral sorption and swelling and potential consequences for CO_2 storage containment and overall trapping potential in storage reservoirs. While we aimed at a general overview of the topic we realise that this research field is still quite immature and requires further work. This is especially true for formations with high smectite contents. We attempted to raise a number of critical issues related to CO_2-clay and CO_2-caprock interactions with the goals of creating awareness and initiating discussions on CO_2-clay interactions that go beyond the laboratory scale. Some of the fundamentals have been addressed in recent work of the authors of this paper or by other researchers. The transfer of these fundamentals into geological applications is recommended for the future and this transfer should mainly address the geological risks of storing CO_2 underneath caprocks with high contents of swelling clays.

The specific aspects addressed here can be summarised as follows: *For reservoir rocks* we find that clay minerals (smectite, illite, kaolinite) can act as a sink for carbon storage by physical adsorption of CO_2. Clays in general have a high specific surface area and it was shown that the sorption capacity correlates well with the supermicropore/mesopores/macropore surface areas determined using N_2 low pressure sorption. The sorptive trapping certainly depends on the overall clay content in the reservoir formation. Considering however a fast reaction rate and potentially comparable trapping capacities in the form of dissolution or mineral trapping, it should be considered in the evaluation of certain storage projects. In addition to reservoir rocks we can state that *for intact caprocks,* fluid transport through the matrix occurs by diffusion only, and little or no leakage is expected. Diffusion-driven sorption increases concentration gradients from the base to the top of the sealing formation. Therefore a slight increase in diffusive fluxes can be expected. Nevertheless, diffusive transport is slow and diffusive leakage is probably irrelevant over time scales of at least thousands of years. Some care should be taken when a dry or near dry CO_2-plume gets in contact with the reservoir/seal interface by buoyancy. Smectite bearing shale could dewater by pore or interlayer water dissolution in CO_2. As a consequence dehydration cracks are plausible; their frequency and propagation into the seal formation depends on diffusion coefficients, plume saturation, seal porosity etc. Another potential leakage mechanism relates to *wellbore annuli* that can develop between cement and host rock following thermal effects or non-perfect cementation. If dry CO_2 is migrating upwards along such an annulus, pore water in the seal will be dissolved and transported to more shallow reservoirs, or to the surface. Similar to the situation for intact seals, this process could lead to dehydration cracks, possibly increasing the leak rates along the well. In contrast to intact seals or wells we expect (partial) healing *of fractures* subject to normal stresses. This is because smectite aligned at the fracture surfaces will swell and lead to decreasing fracture apertures and flux rates. In contrast it was found that clay swelling may result in the development of swelling stresses that under certain circumstances, can potentially lead to shear-type failure. As a consequence faults may get activated if impact area is large enough. However shear-type failure does not necessarily lead to fluid leakage. This depends on many factors, among others the contact area, mineralogy in the fault zone, effective normal stress or reservoir pressurization. Detailed case-by-case investigations are needed for risk assessment of storage sites that are transected by faults.

References

Al Mansoori SK, Itsekiri E, Iglauer S, Pentland CH, Bijeljic B, Blunt MJ (2010) Measurements of non-wetting phase trapping applied to carbon dioxide storage. Int J Greenhouse Gas Control 4:283–288

Altaner SP, Ylagan RF (1997) Comparison of structural models of mixed-layer illite/smectite and reaction mechanisms of smectite illitization. Clays Clay Miner 45:517–533

Amann A, Weniger P, Krooß BM, Littke R, Bertier P, Stanjek H, Draeger I, Clauser C, Blume J, Eckhart J-D, Stosch HG, Neumann T, Mutschler T, Balthasar K, Triantafyllidis T (2011) CO_2 seals—integrity of sealing rock formations for CO_2 storage. BMBF/DFG special program, Geotechnologien

Audigane P, Gaus I, Xu T, Pruess K (2005) Reactive transport modeling using TOUGHREACT for the long term CO_2 storage at Sleipner, North Sea. In: Fourth annual conference on carbon capture and sequestration, Alexandria, VA, p 17

Bachu S, Bennion DB (2009) Experimental assessment of brine and/or CO_2 leakage through well cements at reservoir conditions. Int J Greenhouse Gas Control 3:494–501

Barlet-Gouedard V, Rimmele G, Porcherie O, Quisel N, Desroches J (2009) A solution against well cement degradation under CO_2 geological storage environment. Int J Greenhouse Gas Control 3:206–216

Barton CA, Zoback MD, Moos D (1995) Fluid flow along potentially active faults in crystalline rock. Geology 23:683–686

Bergaya F, Theng BKG, Lagaly G (2006) Handbook of clay science. Dev Clay Sci 1:1224

Bertier P, Schweinar K, Stanjek H, Ghanizadeh A, Clarkson CR, Busch A, Kampman N, Prinz D, Amann-Hildenbrand A, Krooss BM, Pipich V, Di Z (in press) On the use and abuse of N_2 physisorption for the characterization of the pore structure of shales. Clay Clay Miner

Bird P (1984) Hydration-phase diagrams and friction of montmorillonite under laboratory and geologic conditions, with implications for shale compaction, slope stability, and strength of fault gouge. Tectonophysics 107:235–260

Bois A-P, Garnier A, Rodot F, Saint-Marc J, Aimard N (2009) How to prevent loss of zonal isolation through a comprehensive analysis of micro-annulus formation. In: SPE annual conference and exhibition (SPE 124719), New Orleans

Botan A, Rotenberg B, Marry V, Turq P, Noetinger B (2010) Carbon dioxide in montmorillonite clay hydrates: thermodynamics, structure, and transport from molecular simulation. J Phys Chem C 114:14962–14969

Bourg IC (2015) Sealing shales versus brittle shales: a sharp threshold in the material properties and energy technology uses of fine-grained sedimentary rocks. Environ Sci Technol Lett 2:255–259

Brigatti MF, Galan E, Theng BKG (2013) Chapter 2—structure and mineralogy of clay minerals. In: Bergaya F, Lagaly G (eds) Developments in clay science. Elsevier, Amsterdam, pp 21–81

Busch A, Amann-Hildenbrand A (2013) Predicting capillarity of mudrocks. Mar Pet Geol 45:208–223

Busch A, Gensterblum Y (2011) CBM and CO_2-ECBM related sorption processes in coal: a review. Int J Coal Geol 87:49–71

Busch A, Alles S, Gensterblum Y, Prinz D, Dewhurst DN, Raven MD, Stanjek H, Krooss BM (2008) Carbon dioxide storage potential of shales. Int J Greenhouse Gas Control 2:297–308

Busch A, Bertier P, Gensterblum Y, Giesting P, Guggenheim S, van Groos AK, Weniger P (2012) Clay/CO_2 interactions in the context of geological storage of carbon dioxide, 3rd EAGE Shale workshop-shale physics and shale chemistry

Carey JW, Lei Z, Rougier E, Mori H, Viswanathan H (2015) Fracture-permeability behavior of shale. J Unconvent Oil Gas Resourc 11:27–43

Chareonsuppanimit P, Mohammad SA, Robinson RL Jr, Gasem KAM (2012) High-pressure adsorption of gases on shales: measurements and modeling. Int J Coal Geol 95:34–46

Costanzo PA, Guggenheim S (2001) Baseline studies of the clay minerals society source clays. Clays Clay Miner 49:371

Cygan RT, Romanov VN, Myshakin EM (2012) Molecular simulation of carbon dioxide capture by montmorillonite using an accurate and flexible force field. J Phys Chem C 116:13079–13091

de Jong SM, Spiers CJ, Busch A (2014) Development of swelling strain in smectite clays through exposure to carbon dioxide. Int J Greenhouse Gas Control 24:149–161

Duan Z, Sun R (2003) An improved model calculating CO2 solubility in pure water and aqueous NaCl solutions from 273 to 533 K and from 0 to 2000 bar. Chem Geol 193:257–271

Dusseault MB (2011) Geomechanical challenges in petroleum reservoir exploitation. KSCE J Civil Eng 15:669–678

Edwards RWJ, Celia MA, Bandilla KW, Doster F, Kanno CM (2015) A model to estimate carbon dioxide injectivity and storage capacity for geological sequestration in shale gas wells. Environ Sci Technol 49:9222–9229

Espinoza DN, Santamarina JC (2012) Clay interaction with liquid and supercritical CO_2: the relevance of electrical and capillary forces. Int J Greenhouse Gas Control 10:351–362

Ferrage E, Lanson B, Michot LJ, Robert J-L (2010) Hydration properties and interlayer organization of water and ions in synthetic Na-smectite with tetrahedral layer charge. Part 1. Results from X-ray diffraction profile modeling. J Phys Chem C 114:4515–4526

Ferrage E, Vidal O, Mosser-Ruck RG, Cathelineau M, Cuadros J (2011) A reinvestigation of smectite illitization in experimental hydrothermal conditions: results from X-ray diffraction and transmission electron microscopy. Am Mineral 96:207–223

Fitts JP, Peters CA (2013) Caprock fracture dissolution and CO_2 leakage. Rev Mineral Geochem 77:459–479

Fjær E, Holt RM, Horsrud P, Raaen AM, Risnes R (2008) Petroleum related rock mechanics, 2nd edn

Foerster A, Schoener R, Foerster HJ, Norden B, Blaschke AW, Luckert J, Beutler G, Gaupp R, Rhede D (2010) Reservoir characterization of a CO_2 storage aquifer: the upper Triassic Stuttgart formation in the Northeast German Basin. Mar Pet Geol 27:2156–2172

Fripiat JJ, Cruz ML, Bohor BF, Thomas J Jr (1974) Interlamellar adsorption of carbon dioxide by smectites. Clays Clay Miner 22:23–30

Gasda SE, Bachu S, Celia MA (2004) Spatial characterization of the location of potentially leaky wells penetrating a deep saline aquifer in a mature sedimentary basin. Environ Geol 46:707–720

Gensterblum Y, van Hemert P, Billemont P, Busch A, Charriere D, Li D, Krooss BM, de Weireld G, Prinz D, Wolf KHAA (2009) European inter-laboratory comparison of high pressure CO2 sorption isotherms. I: activated carbon. Carbon 47:2958–2969

Gensterblum Y, van Hemert P, Billemont P, Battistutta E, Busch A, Krooss BM, De Weireld G, Wolf KHAA (2010)

European inter-laboratory comparison of high pressure CO_2 sorption isotherms II: natural coals. Int J Coal Geol 84:115–124

Gensterblum Y, Merkel A, Busch A, Krooss BM, Littke R (2014) Gas saturation and CO_2 enhancement potential of coalbed methane reservoirs as a function of depth. AAPG Bull 98:395–420

Giesting P, Guggenheim S, Koster van Groos AF, Busch A (2012a) Interaction of carbon dioxide with Na-exchanged montmorillonite at pressures to 640 bars: implications for CO_2 sequestration. Int J Greenhouse Gas Control 8:73–81

Giesting P, Guggenheim S, Koster van Groos AF, Busch A (2012b) X-ray diffraction study of K- and Ca-exchanged montmorillonites in CO_2 atmospheres. Environ Sci Technol 46:5623–5630

Godec M, Koperna G, Petrusak R, Oudinot A (2013) Potential for enhanced gas recovery and CO_2 storage in the Marcellus Shale in the Eastern United States. Int J Coal Geol 118:95–104

Hangx S, van der Linden A, Marcelis F, Bauer A (2013) The effect of CO_2 on the mechanical properties of the Captain Sandstone: geological storage of CO_2 at the Goldeneye field (UK). Int J Greenhouse Gas Control 19:609–619

Hower J, Eslinger EV, Hower ME, Perry EA (1976) Mechanism of burial metamorphism of argillaceous sediment: 1. mineralogical and chemical evidence. Geol Soc Am Bull 87:725–737

Hur T-B, Baltrus JP, Howard BH, Harbert WP, Romanov VN (2013) Carbonate formation in Wyoming montmorillonite under high pressure carbon dioxide. Int J Greenhouse Gas Control 13:149–155

Iglauer S, Wülling W, Pentland CH, Mansoori SKA, Blunt MJ (2009) Capillary trapping capacity of rocks and sandpacks, EUROPEC/EAGE conference and exhibition. Society of Petroleum Engineers, Amsterdam

Iglauer S, Pentland CH, Busch A (2015) CO2 wettability of seal and reservoir rocks and the implications for carbon geo-sequestration. Water Resour Res 51:729–774

Ilton ES, Schaef HT, Qafoku O, Rosso KM, Felmy AR (2012) In situ X-ray diffraction study of Na^+ saturated montmorillonite exposed to variably wet super critical CO_2. Environ Sci Technol 46:4241–4248

Jeon PR, Choi J, Yun TS, Lee C-H (2014) Sorption equilibrium and kinetics of CO_2 on clay minerals from subcritical to supercritical conditions: CO_2 sequestration at nanoscale interfaces. Chem Eng J 255:705–715

Kang SM, Fathi E, Ambrose RJ, Akkutlu IY, Sigal RF (2010) CO_2 storage capacity of organic-rich shales. In: SPE annual technical conference and exhibition. Society of Petroleum Engineers, Florence

Khosrokhavar R, Griffiths S, Wolf K-H (2014) Shale gas formations and their potential for carbon storage: opportunities and outlook. Environ Process 1:595–611

Krooss BM, Leythaeuser D, Schaefer RG (1992) The quantification of diffusive hydrocarbon losses through cap rocks of natural gas reservoirs—a reevaluation. AAPG Bull 76:403–406

Krukowski EG, Goodman A, Rother G, Ilton ES, Guthrie G, Bodnar RJ (2015) FT-IR study of CO_2 interaction with Na^+ exchanged montmorillonite. Appl Clay Sci 114:61–68

Lanson B, Sakharov BA, Claret F, Drits VA (2009) Diagenetic smectite-to-illite transition in clay-rich sediments: a reappraisal of X-ray diffraction results using the multi-specimen method. Am J Sci 309:476–516

Li X, Elsworth D (2014) Geomechanics of CO_2 enhanced shale gas recovery. J Nat Gas Sci Eng doi:10.1016/j.jngse.2014.08.010

Liu F, Ellett K, Xiao Y, Rupp JA (2013) Assessing the feasibility of CO_2 storage in the New Albany Shale (Devonian-Mississippian) with potential enhanced gas recovery using reservoir simulation. Int J Greenhouse Gas Control 17:111–126

Loizzo M, Akemu OA, Jammes L, Desroches J, Lombardi S, Annunziatellis A (2011) Quantifying the risk of CO_2 leakage through wellbores. Society of Petroleum Engineers SPE-139635-PA

Loring JS, Thompson CJ, Wang Z, Joly AG, Sklarew DS, Schaef HT, Ilton ES, Rosso KM, Felmy AR (2011) In situ infrared spectroscopic study of forsterite carbonation in wet supercritical CO_2. Environ Sci Technol 45:6204–6210

Loring JS, Schaef HT, Turcu RVF, Thompson CJ, Miller QRS, Martin PF, Hu J, Hoyt DW, Qafoku O, Ilton ES, Felmy AR, Rosso KM (2012) In situ molecular spectroscopic evidence for CO_2 intercalation into montmorillonite in supercritical carbon dioxide. Langmuir 28:7125–7128

Loring JS, Ilton ES, Chen J, Thompson CJ, Martin PF, Benezeth P, Rosso KM, Felmy AR, Schaef HT (2014) In situ study of CO_2 and H_2O partitioning between Na-montmorillonite and variably wet supercritical carbon dioxide. Langmuir 30:6120–6128

Meunier A (2005) Clays. Springer, Heidelberg

Mohajerani M, Delage P, Sulem J, Monfared M, Tang AM, Gatmiri B (2012) A laboratory investigation of thermally induced pore pressures in the Callovo-Oxfordian claystone. Int J Rock Mech Min Sci 52:112–121

Mohajerani M, Delage P, Sulem J, Monfared M, Tang A, Gatmiri B (2014) The thermal volume changes of the callovo-oxfordian claystone. Rock Mech Rock Eng 47:131–142

Monfared M, Sulem J, Delage P, Mohajerani M (2011) A laboratory investigation on thermal properties of the opalinus claystone. Rock Mech Rock Eng 44:735–747

Myshakin EM, Saidi WA, Romanov VN, Cygan RT, Jordan KD (2013) Molecular dynamics simulations of carbon dioxide intercalation in hydrated Na-montmorillonite. J Phys Chem C 117:11028–11039

Myshakin EM, Makaremi M, Romanov VN, Jordan KD, Guthrie GD (2014) Molecular dynamics simulations of turbostratic dry and hydrated montmorillonite with intercalated carbon dioxide. J Phys Chem A 118(35):7454–7468. doi:10.1021/jp500221w

Nuttall BC, Drahovzal JA, Eble CF, Bustin RM (2009) Regional assessment of suitability of organic-rich shales for carbon sequestration: an example from the devonian shales of the Illinois and Appalachian Basins, Kentucky. In: Grobe M, Pashin JC, Dodge RL (eds) Carbon dioxide sequestration in geological media-state of science. AAPG Stud Geol, pp 173–190

Pearson MJ (1990) Clay mineral distribution and provenance in Mesozoic and Tertiary mudrocks of the Moray Firth and northern North Sea. Clay Miner 25:519–541

Reeves S (2001) Geological sequestration of CO_2 in deep, unmineable coalbeds: an integrated research and

commerical-scale field demonstration project. SPE J 71749:1–11

Reiss LH (1980) The reservoir engineering aspects of fractures reservoirs. Institut Francaise du Petrole

Romanov VN (2013) Evidence of irreversible CO_2 intercalation in montmorillonite. Int J Greenhouse Gas Control 14:220–226

Rother G, Ilton ES, Wallacher D, Hauss T, Schaef HT, Qafoku O, Rosso KM, Felmy AR, Krukowski EG, Stack AG, Grimm N, Bodnar RJ (2013a) CO2 sorption to subsingle hydration layer montmorillonite clay studied by excess sorption and neutron diffraction measurements. Environ Sci Technol 47:205–211

Rother G, Krukowski EG, Wallacher D, Grimm N, Bodnar RJ, Cole DR (2013b) Pore size effects on the sorption of supercritical CO_2 in mesoporous CPG-10 silica. J Phys Chem C 116:917–922

Samuelson J, Spiers CJ (2012) Fault friction and slip stability not affected by CO_2 storage: evidence from short-term laboratory experiments on North Sea reservoir sandstones and caprocks. Int J Greenhouse Gas Control 11(Supplement):S78–S90

Schaef HT, Ilton ES, Qafoku O, Martin PF, Felmy AR, Rosso KM (2012) In situ XRD study of Ca^{2+} saturated montmorillonite (STX-1) exposed to anhydrous and wet supercritical carbon dioxide. Int J Greenhouse Gas Control 6:220–229

Schaef HT, Loring JS, Glezakou V-A, Miller QRS, Chen J, Owen AT, Lee M-S, Ilton ES, Felmy AR, McGrail BP, Thompson CJ (2015) Competitive sorption of CO_2 and H_2O in 2:1 layer phyllosilicates. Geochim Cosmochim Acta 161:248–257

Schlömer S, Krooss BM (1997) Experimental characterisation of the hydrocarbon sealing efficiency of cap rocks. Mar Pet Geol 14:565–580

Schlömer S, Krooss BM (2004) Molecular transport of methane, ethane nd nitrogene and the influence of diffusion on the chemical and isotopic composition of natural gas accumulations. Geofluids 4:81–108

Siemons N, Busch A (2007) Measurement and interpretation of supercritical CO_2 sorption on various coals. Int J Coal Geol 69:229–242

Snippe J, Wei L, Tucker O (2012) Containment impact of calcite pathways in the primary caprock of CO_2 storage in a depleted North Sea gas field. In 11th greenhouse gas technology conference, Kyoto

Span R, Wagner W (1996) A new equation of state for carbon dioxide covering the fluid region from the triple-point temperature to 1100 K at pressures up to 800 MPa. J Phys Chem Ref Data 25:1509–1596

Spiering P, Wentinck R, Busch A, Fraaije JGEM, Tambach TJ (2014) Molecular mechanisms of CO_2 in swelling clays, Goldschmidt 2014, Sacramento

Spycher N, Pruess K, Ennis-King J (2003) CO2-H2O mixtures in the geological sequestration of CO_2. I. Assessment and calculation of mutual solubilities from 12 to 100°C and up to 600 bar. Geochim Cosmochim Acta 67:3015–3031

Tao Z, Clarens A (2013) Estimating the carbon sequestration capacity of shale formations using methane production rates. Environ Sci Technol 47:11318–11325

Thomas J Jr, Bohor BF (1968) Surface area of montmorillonite from the dynamic sorption of nitrogen and carbon dioxide. Clays Clay Miner 16:83–91

Thommes M, Kaneko K, Neimark Alexander V, Olivier James P, Rodriguez-Reinoso F, Rouquerol J, Sing Kenneth SW (2015) Physisorption of gases, with special reference to the evaluation of surface area and pore size distribution (IUPAC Technical Report), Pure and Applied Chemistry, p 1051

Townend J, Zoback MD (2000) How faulting keeps the crust strong. Geology 28:399–402

van Bergen F, Pagnier H, Krzystolik P (2006) Field experiment of enhanced coalbed methane-CO_2 in the Upper Silesian basin of Poland. Environ Geosci 13:201–224

van Oort E (2003) On the physical and chemical stability of shales. J Petrol Sci Eng 38:213–235

Velde B, Vasseur G (1992) Estimation of the diagenetic smectite top illite trans-formation in time-temperature space. Am Mineral 77:967–976

Wang Y, Papamichos E, Dusseault MB (1996) Thermal stresses and borehole stability. A.A. Balkema. Permission to Distribute—American Rock Mechanics Association

Weniger P, Kalkreuth W, Busch A, Krooss BM (2010) High-pressure methane and carbon dioxide sorption on coal and shale samples from the Paraná Basin, Brazil. Int J Coal Geol 84:190–205

Wentinck HM, Busch A (2014) The swelling of smectites by high-pressure CO_2 and the possible impact on the containment of CO_2 below the caprock, Mid European clay conference, Dresden

Xu T, Kharaka YK, Doughty C, Freifeld BM, Daley TM (2010) Reactive transport modeling to study changes in water chemistry induced by CO_2 injection at the Frio-I Brine Pilot. Chem Geol 271:153–164

Zhang M, Spiers CJ, Busch A, Wentinck R (2014) Swelling stress development in smectites upon exposure to CO_2 under in situ P-T conditions. In: Mid European clay conference, Dresden